

Theory of Magnetic Confinement of Massless Dirac Fermions in Graphene

Joshua Loizou, Supervisors: Misha Portnoi and Eros Mariani

15th March 2020

Massless Dirac fermions in graphene exhibit the phenomenon of Klein tunneling when incident to a potential barrier, in which relativistic particles pass through the barrier with no decay in wavefunction amplitude. Electric fields are therefore not adequate for quantum confinement of such particles. Non-uniform magnetic fields may be used to facilitate confined transport of charge carriers over a graphene sheet in the form of snake states. Here presented is the background theory of the emergence of the aforementioned phenomena and other required theory to explore snake state confinement using the magnetic field produced by a uniform current loop.

1 Introduction

Graphene is an allotrope of carbon consisting of monoatomic thick sheet of carbon atoms. The study of graphene can be traced back as far as 1947 when Wallace considered single graphite sheets as a starting point for theoretical studies of the electronic properties of graphite [1]. Since then this research area remained relatively inactive until 2004 when Geim and Novoselov exfoliated high quality samples of graphene using the micro-mechanical cleavage method[2]. The relative ease of obtaining samples of graphene made it a good candidate for theoretical and experimental study, resulting a rapid growth of this field in the condensed matter community.

The two dimensional structure of graphene gives emergence of Klein tunneling in the material [3] wherein relativistic electrons travel through potential barriers unimpeded. While this phenomenon may be exploited for many applications, in the realm of graphene based electronics this does provide a limitation, in that precise control of electron transport in graphene sheets currently unobtainable.

Magnetic fields provide a solution to this issue as the action of a magnetic field on a charged particle fundamentally changes its canonical momentum, unlike electric fields. Uniform magnetic fields do confine electrons in graphene, however these result in microscopic closed electron orbits so are not useful for the application of electron transport. Therefore the aim is to build on current ongoing research using realistic non-uniform magnetic fields to control electron transport within graphene monolayers, starting with a uniform current loop.

2 Background Theory

2.1 Graphene Crystal Structure

2.1.1 Real Space Structure

Graphene has a crystal structure of two superimposed hexagonal lattices [1] as shown in Figure 1. These sublattices are identical other than a relative rotation of π radians. Figure 1 shows the two sublattices and how the lattice vectors are defined for this work..

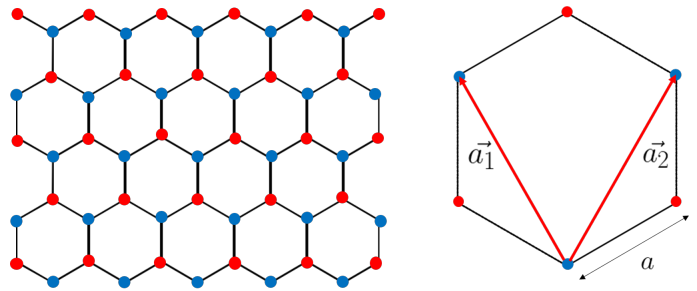


Figure 1: [Left]: A diagram of the hexagonal crystal structure of graphene, with the two distinct sublattices being shown as red and blue points on a honeycomb. [Right]: The lattice vectors for one of the hexagonal lattices where a is the nearest neighbour distance ($a = 1.42$ Å)[4].

One can show simply the lattice vectors, in this orientation, are:

$$\vec{a}_1 = \frac{a}{2} (-\sqrt{3}, 3); \vec{a}_2 = \frac{a}{2} (\sqrt{3}, 3) \quad (1)$$

2.1.2 Momentum Space Structure

By using the standard formulae for reciprocal space vectors, the reciprocal lattice vectors of graphene are found to be:

$$\vec{b}_1 = \left(-\frac{2\pi}{\sqrt{3}a}, \frac{2\pi}{3a} \right); \vec{b}_2 = \left(\frac{2\pi}{\sqrt{3}a}, \frac{2\pi}{3a} \right) \quad (2)$$

Which may be used to locate the \vec{K} and \vec{K}' symmetry points of the reciprocal lattice as shown in Figure 2:

$$\vec{K} = \left(\frac{4\pi}{3a\sqrt{3}}, 0 \right); \vec{K}' = \left(-\frac{4\pi}{3a\sqrt{3}}, 0 \right) \quad (3)$$

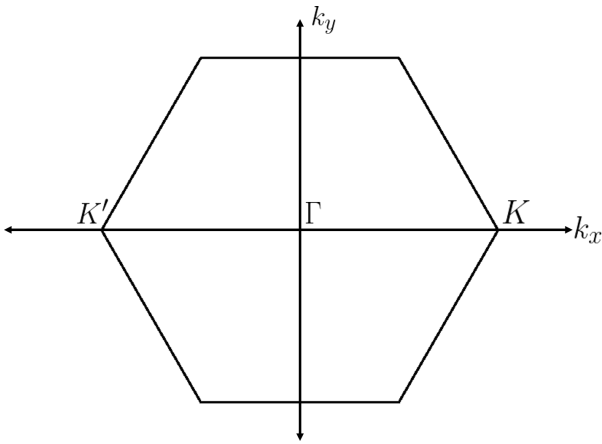


Figure 2: The First Brillouin zone of the sublattices shown in Figure 1. Due to the rotation of π radians differing the two sublattices, one can see that rotating the First Brillouin Zone by π radians results in the same Brillouin zone, meaning that each real space lattice produces the same momentum space lattice.

2.2 Graphene Monolayer Band Structure

2.2.1 Carbon Electronic Structure

Carbon has an outer atomic structure of $2s^22p^2$. In graphene the the $2p_x$ and $2p_y$ orbitals hybridise with the $2s$ orbital to form 3 sp^2 orbitals per carbon atom, with an outer electron occupying each orbital at an angular separation of $\frac{\pi}{3}$ radians. Outer electrons of neighbouring atomic sites share these orbitals forming 3 σ bonds per atom giving the “honeycomb” structure as seen in Figure 1. This leaves a single π state electron per atom, which is delocalised over the graphene crystal structure[6]. It is the gas of these π state electrons which is the focus study.

2.2.2 Tight-binding Model

By simple inspection one can see that the crystal structure of graphene is periodic in nature, and hence the potential induced by the atomic sites is also; it has the form $V(\vec{r}) = V(\vec{r} - \vec{R}_{\{j\}})$ where $R_{\{j\}}$ is the lattice translation vector. Note that a wavefunction satisfying a periodic potential has the form [7] (a Bloch summation):

$$|\Psi(\vec{r}, \vec{k})\rangle = \frac{1}{\sqrt{N}} \sum_{\{j\}} e^{i\vec{k}\cdot(\vec{r} - \vec{R}_{\{j\}})} |\phi(\vec{r} - \vec{R}_{\{j\}})\rangle \quad (4)$$

Where $|\phi(\vec{r})\rangle = |\phi(\vec{r} - \vec{R}_{\{j\}})\rangle$ is the on site wavefunction, N is the total number of unit cells.

In our case with two sublattices in two dimensions this becomes:

$$|\Psi(\vec{r}, \vec{k})\rangle = \frac{c_A(\vec{k})}{N_A} \sum_{n,m} e^{i\vec{k}\cdot(n\vec{a}_1 + m\vec{a}_2)} |\phi_A(\vec{r} - n\vec{a}_1 - m\vec{a}_2)\rangle + \frac{c_B(\vec{k})}{N_B} \sum_{n,m} e^{i\vec{k}\cdot(n\vec{a}_1 + m\vec{a}_2)} |\phi_B(\vec{r} - n\vec{a}_1 - m\vec{a}_2)\rangle \quad (5)$$

Where $c_A(\vec{k})$ and $c_B(\vec{k})$ are the amplitudes which give the probability of finding an electron lying on the A or B sublattice respectively. Equation (6) may be written as $|\Psi(\vec{r}, \vec{k})\rangle = c_A(\vec{k}) |\Phi_A(\vec{r}, \vec{k})\rangle + c_B(\vec{k}) |\Phi_B(\vec{r}, \vec{k})\rangle$ for conciseness.

The time-independent Schrödinger equation is:

$$\hat{\mathcal{H}} |\Psi(\vec{r}, \vec{k})\rangle = E |\Psi(\vec{r}, \vec{k})\rangle \quad (6)$$

Subbing in our Bloch summation we eventually arrive at:

$$|\hat{H}_{ij}(\vec{r}, \vec{k}) - EI| = 0 \quad (7)$$

Where $\hat{H}_{ij}(\vec{r}, \vec{k}) = \langle \Phi_i(\vec{r}, \vec{k}) | \hat{\mathcal{H}} | \Phi_j(\vec{r}, \vec{k}) \rangle$ and ij (i.e., AA, AB, BA and BB) labels label combinations of the sublattices. Following from Equation (7) one finds the matrix elements may be written as:

$$\hat{H}_{ij}(\vec{r}, \vec{k}) = \sum_{n,m} e^{i\vec{k}\cdot(n\vec{a}_1 + m\vec{a}_2)} \langle \phi_i(\vec{r}) | \hat{\mathcal{H}} | \phi_j(\vec{r} - n\vec{a}_1 - \vec{a}_2) \rangle \quad (8)$$

Now the tight binding model is used, in that only electron hopping within an unit cell and the nearest two neighbours of said unit cell is considered. To do this, say for the matrix element \hat{H}_{AB} , take only the first three terms in the summation in Equation (8) (the terms corresponding to $n = m = 0$; $n = 0, m = 1$ and $n = 1, m = 0$) giving the matrix element as:

$$\begin{aligned} \hat{H}_{AB}(\vec{r}, \vec{k}) &= \langle \phi_A(\vec{r}) | \hat{\mathcal{H}} | \phi_B(\vec{r}) \rangle \\ &+ e^{i\vec{k}\cdot\vec{a}_1} \langle \phi_A(\vec{r}) | \hat{\mathcal{H}} | \phi_B(\vec{r} - \vec{a}_1) \rangle \\ &+ e^{i\vec{k}\cdot\vec{a}_2} \langle \phi_A(\vec{r}) | \hat{\mathcal{H}} | \phi_B(\vec{r} - \vec{a}_2) \rangle \end{aligned} \quad (9)$$

Calling the on site wavefunction overlap integrals the hopping parameter t , our matrix element is found as a function of wavevector only:

$$\hat{H}_{AB}(\vec{k}) = t(1 + \sum_j e^{i\vec{k}\cdot\vec{a}_j}) = tS(\vec{k}) \quad (10)$$

2.2.3 Electronic Dispersion

Now the Hamiltonian may be constructed using the matrix element given in Equation (10) and the Hermitian conjugateness of quantum mechanical operators to give the Hamiltonian as:

$$\hat{H} = \begin{pmatrix} 0 & tS(\vec{k}) \\ tS^*(\vec{k}) & 0 \end{pmatrix} \quad (11)$$

where the entire spectrum has been shifted by the onsite energy given by the elements $\hat{H}_{AA/BB}(\vec{r}) = \langle \phi_{A/B}(\vec{r}) | \hat{\mathcal{H}} | \phi_{A/B}(\vec{r}) \rangle$ so that the diagonals of the Hamiltonian are zero. This has no effect on the physics of the problem but simplifies the mathematics. If the characteristic equation of Hamiltonian (11) is solved one arrives at the following dispersion relation:

$$E(\vec{k}) = \sqrt{1 + f(\vec{k})} \quad (12)$$

where $f(\vec{k})$ is given by:

$$f(\vec{k}) = 2 \cos(k_y a) + 4 \cos\left(\frac{\sqrt{3}}{2} k_y a\right) \cos\left(\frac{3}{2} k_x a\right) \quad (13)$$

A plot of this dispersion relation can be seen in Figure 3.

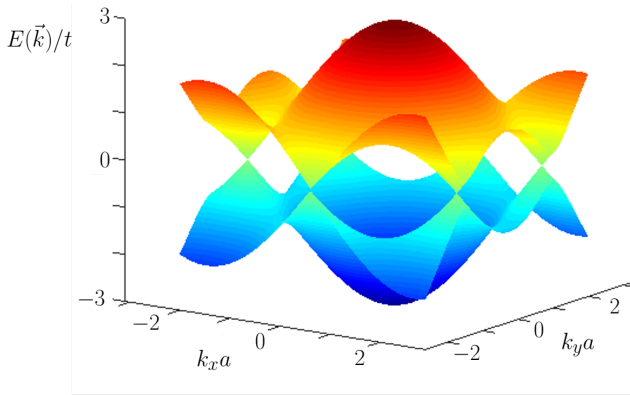


Figure 3: A plot of the dispersion relation of graphene. The orange region corresponds to the conduction band and the blue to the valence band. The Fermi energy is at the zero energy level, where the two bands ‘touch’. One can see from this plot that graphene is a zero band gap semiconductor. If one looks around the regions where the two bands meet one can clearly see the deviation from parabolic dispersion to linear dispersion.

One novel feature of note of this plot is around the \vec{K} and \vec{K}' points the dispersion appears to be linear, unlike the parabolic dispersion found in most materials. These linear regions of linear dispersion are called the “Dirac Cones”[9]. Let us explore the behaviour around these points further.

2.3 Massless Dirac Fermions

Taking the Hamiltonian in Equation (11) and making a Taylor expansion around the \vec{K} point, one yeilds:

$$\hat{H}_{\vec{K}} = \hbar v_F \begin{pmatrix} 0 & q_x - iq_y \\ q_x + iq_y & 0 \end{pmatrix} \quad (14)$$

Where $\vec{q} = \vec{k} - \vec{K}$ is the distance of the electron in momentum space from \vec{K} point and v_F is the Fermi velocity. In this calculation we have identified the relation that $\frac{3}{2}at = \hbar v_F$. Repeating this analysis for behaviour around the \vec{K}' shows $\hat{H}_{\vec{K}'} = \hat{H}_{\vec{K}}^T$. These may be written together as one 4×4 matrix but for simplicity’s sake we will deal with these as two separate blocks.

Again, solving the characteristic equation for the Hamiltonian (14) around these points we arrive at the following dispersion relation:

$$E(\vec{q}) = \hbar v_F |\vec{q}| \quad (15)$$

Making a comparison to the well-known dispersion relation of relativistic particles: $E(\vec{q}) = \sqrt{\hbar^2 c^2 |\vec{q}|^2 + m^2 c^4}$

It can be seen that the dispersion relation in Equation (15) mirrors that of a relativistic particle with no rest mass moving at the Fermi velocity, which in graphene is $\approx 10^6$ m.s⁻¹[10]. It is the relativistic nature of electrons in graphene that gives rise to many of its novel properties. Particles behaving in this way are referred to as “massless Dirac fermions”[11]. Particles behaving in such a manner should be considered with a full relativistic treatment.

2.4 Spinors

Now the energetic behaviour of the electrons in graphene has been explored, to progress further it is instructive to investigate the nature of the wavefunction of these particles before progressing further. Recalling the Hamiltonian in Equation (11), an intermediate step between this and yielding Equation (12) is:

$$E(\vec{k}) = \pm t |S(\vec{k})| \quad (16)$$

considering a generic two component wave function of the form $|\Psi\rangle = \begin{pmatrix} \psi_A \\ \psi_B \end{pmatrix}$ we may write

$$\begin{pmatrix} 0 & S(\vec{k}) \\ S^*(\vec{k}) & 0 \end{pmatrix} \begin{pmatrix} \psi_A \\ \psi_B \end{pmatrix} = |S(\vec{k})| \begin{pmatrix} \psi_A \\ \psi_B \end{pmatrix} \quad (17)$$

Where the common factor of t on both sides of this relation has been canceled. From this we obtain a system of linear equations, taking one of these we have:

$$\pm |S(\vec{k})| \psi_A = S(\vec{k}) \psi_B \quad (18)$$

From Equation (16) one can see that if one cancels the magnitude of the complex valued function $S(\vec{k})$ the components of the wavefunction are equal in magnitude and differ only by a phase factor. Setting $\psi_B = 1$, after normalisation the wavefunction has the form:

$$|\Psi\rangle = \frac{1}{\sqrt{2}} \begin{pmatrix} \pm e^{i\theta(\vec{k})} \\ 1 \end{pmatrix} \quad (19)$$

Such wavefunctions are referred to as “spinors”. Wavefunctions of this form appear in quantum field theories [12] in which particles are treated using relativistic fields. This provides further evidence that the physics of particles in graphene is relativistic in nature. Here it is interesting to note that graphene shows that the simple imposition of a periodic potential causes electrons to behave as if they are high energy particles.

2.5 Klein Tunnelling

The Dirac equation governs the dynamics of relativistic quantum particles [13]. Soon after Dirac completed this work Klein considered the familiar problem of a quantum particle impinging upon a potential barrier[14], and it was found that the wavefunction of the particle experienced no decay in the barrier, unlike in the non-relativistic case as seen in Figure 4. In Klein tunneling the wavefunction in the barrier is a plane wave (for the three dimensional case) meaning the particle has an equal probability of being found outside the barrier to inside the barrier. This causes the result that when a flux of particles are incident to a potential barrier the transmission coefficient is unitary.

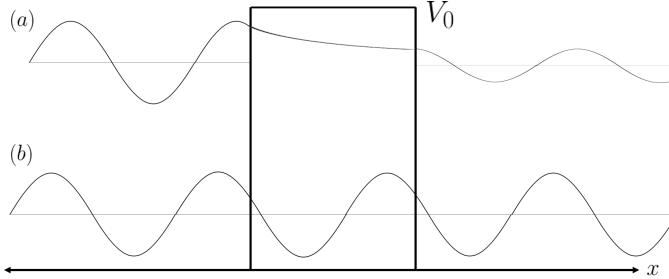


Figure 4: (a): A non-relativistic particle impinging upon a potential barrier. The wavefunction decays in amplitude while in the barrier region and at the far edge of the barrier the amplitude of the wavefunction here becomes maximum amplitude to the right of the barrier. (b): A depiction of Klein tunneling for relativistic particles. One can see there is no decrease in amplitude of the wavefunction within the barrier in this case.

Let us show this for a massless Dirac fermion in one dimension. Introducing an arbitrary potential $V(\vec{r})$ and noting that the Hamiltonian (11) may be rewritten in terms of the Pauli matrices and rewriting the wavevector in its operator form we have:

$$\hat{H} = \hbar v_F \sigma \nabla + V(\vec{r}) \mathbf{I} \quad (20)$$

For simplicity let us reduce this to a one dimensional problem so that the Hamiltonian is:

$$\hat{H} = \hbar v_F \begin{pmatrix} \nu(x) & -i \frac{\partial}{\partial x} \\ -i \frac{\partial}{\partial x} & \nu(x) \end{pmatrix} \quad (21)$$

where we have let $q_x = -i \frac{\partial}{\partial x}$ and introduced the dimensionless variable $\nu(x) = \frac{V(x)}{\hbar v_F}$. Using this, the time-independent Schrödinger equation and a two component wavefunction $|\Psi\rangle = \begin{pmatrix} \psi_A \\ \psi_B \end{pmatrix}$ one arrives at a pair of coupled differential equations:

$$-i \frac{\partial \psi_A}{\partial x} + (\nu(x) - \epsilon) \psi_B = 0 \quad (22)$$

$$-i \frac{\partial \psi_B}{\partial x} + (\nu(x) - \epsilon) \psi_A = 0 \quad (23)$$

Where we have introduced another dimensionless variable $\epsilon = \frac{E}{\hbar v_F}$. Adding together Equations (22) and (23) yeilds:

$$i \frac{\partial \Psi_+}{\partial x} = (\nu(x) - \epsilon) \Psi_+ \quad (24)$$

where $\Psi_+ = \psi_A + \psi_B$. This equation has the solution:

$$\Psi_+ = \Psi_0 \exp \left(-i \int_0^x \nu(x') dx' \right) \exp(i\epsilon x) \quad (25)$$

Recalling the definition of Ψ_+ it can be seen that both components of the spinor wavefunction within an arbitrary potential has the form of a plane wave, due to the final factor in Equation (25), not a evanescent wave as in the non-relativistic, massive case.

This has also been shown to be the case for two dimensional massless Dirac fermions in graphene theoretically [3] and experimentally [15]

Herein lies the crux of the problem of this project: Electrons near the Fermi energy in graphene cannot be confined using electric fields, providing a huge limitation in the field of graphene based electronics. Therefore we must consider other techniques for confinement of these particles; as we shall see a good candidate is the use of magnetic fields.

2.6 Effect of Magnetic Fields - Landau Levels

By considering the Lagrangian of a charged quantum particle in a magnetic field the canonical momentum operator $\hat{\pi}$ is given as[16]:

$$\hat{\pi} = \hat{p} - \frac{e}{c} \hat{A} \quad (26)$$

Where \hat{p} is the kinetic momentum of the particle and \hat{A} is the vector potential of the magnetic field. It can be seen the action of a magnetic field fundamentally alters the canonical momentum of the particle, unlike an electrostatic field, giving us an indication they may be viable for Dirac fermion confinement.

Before the behaviour of massless Dirac fermions in non-uniform magnetic fields is explored it would be sensible to first look at the effect of a uniform magnetic field. Using our new definition of momentum given above and Equation (20) we may write the Hamiltonian as:

$$\hat{H} = v_F \sigma \cdot \hat{\vec{\pi}} \quad (27)$$

Giving the time-independent Schrödinger equation as:

$$v_F \begin{pmatrix} 0 & p_x - \frac{e}{c} A_x - i(p_y - \frac{e}{c} A_y) \\ (p_x - \frac{e}{c} + i(p_y - \frac{e}{c} A_y)) & 0 \end{pmatrix} \cdot \begin{pmatrix} \psi_A \\ \psi_B \end{pmatrix} = E \begin{pmatrix} \psi_A \\ \psi_B \end{pmatrix} \quad (28)$$

Where p_x and p_y are the x and y components of the kinetic momentum respectively. Which leads to the pair of coupled differential equations:

$$v_F \left(-i\hbar \frac{\partial}{\partial x} - eBy - \hbar \frac{\partial}{\partial y} \right) \psi_B = E\psi_A \quad (29)$$

and

$$v_F \left(-i\hbar \frac{\partial}{\partial x} - eBy + \hbar \frac{\partial}{\partial y} \right) \psi_A = E\psi_B \quad (30)$$

where we have let $p_x = -i\hbar \frac{\partial}{\partial x}$, $p_y = -i\hbar \frac{\partial}{\partial y}$. In these equations it is assumed that the magnetic field is orthogonal to the plane of the graphene sheet so the Landau gauge is used, $\vec{A} = (-By, 0, 0)$ [17], where B is the magnitude of the magnetic field.

These equations may be decoupled by simply putting one into the other and rearranging. By using the fact that the system is invariant along the x axis we may introduce a plane wave ansatz along this direction so the x momentum operator may be replaced with its eigenvalue.

This gives two second order differential equations, one for each component of the spinor, which eventually leads to the two energy spectra:

$$E_A = \pm v_F \sqrt{\frac{2e\hbar B}{c}(n+1)} \quad (31)$$

and

$$E_B = \pm v_F \sqrt{\frac{2e\hbar B}{c}n} \quad (32)$$

Which are the Landau levels of graphene, where $n \in \mathbb{Z}$. Comparing to the Landau levels of massive particles: $E_n = \hbar\omega_c(n + \frac{1}{2})$, where ω_c is the cyclotron frequency, one can see that in our case the Landau levels are not evenly spaced as in the conventional case. We can see that our continuous energy spectrum has now become quantised and highly degenerate due the effect of the magnetic field. It can be seen that an increase in magnitude of the magnetic field increases the spacing between these levels. This quantisation of energetic states has been shown to have an important role to play in many physical properties of materials, such as the quantum hall effect[18]. Therefore it will be important to consider the properties of the Landau levels of massless Dirac fermions in non-uniform magnetic fields, and the resultant physics as this will give us key insight into experimentally observable properties which may be used to validate the existence of the confined states this work finds.

3 Future Plans

Current work involves the use of so called “snake-states” to confine graphene electrons[19] [20] [21]. A semi-classical depiction of which can be found in Figure 5. If we can create neighboring regions of continuous magnetic fields orientated in opposite directions we may create a region where the magnetic field is zero[22]. The well known Lorentz force on a charged particle is given (classically) as:

$$\vec{F} = g(\vec{E} + \vec{v} \times \vec{B}) \quad (33)$$

Where \vec{E} is the electric field, \vec{v} is the particle velocity and g its charge. It can be seen if an electron is placed near the region where $\vec{B} = 0$ and given the particle an initial velocity there will be a force orthogonal to this velocity, causing motion to the region where $\vec{B} = 0$. When the particle reaches this region the momentum of the particle will carry it into the region where the direction of the magnetic field is opposite, hence once in this region the particle will again move towards the region where there is no net magnetic field. This motion repeats allowing guided transport of electrons centred on the zero field region.

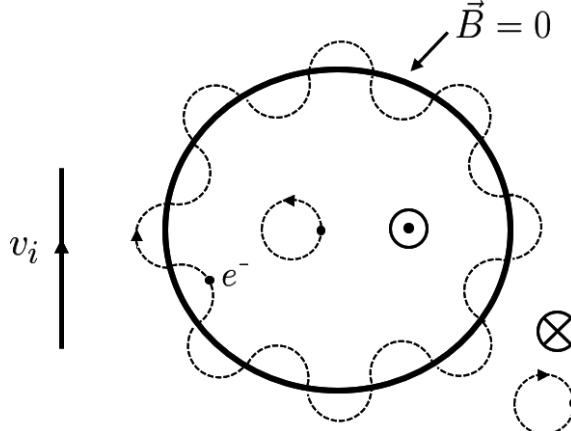


Figure 5: A semi-classical depiction of snake snakes in non-uniform magnetic field. If an electron is far from the field and given an initial velocity the motion of a charged particle in a magnetic field causes a resultant force on the particle. Far from the region where $\vec{B} = 0$ electrons move in microscopic closed orbits, which are confined states, but not useful for electron transport. However if the electron is near the $\vec{B} = 0$ region there is motion centred on the region where $\vec{B} = 0$.

A method of producing the form of magnetic field shown in Figure 5 is to place a current loop above a sheet of graphene. If one considers the form of the magnetic field resulting from a current loop it can be seen around the band of the loop, above and below, the field lines are pointing in opposite directions thus cancel out, giving a line of zero magnetic field. This means that either side of this line the magnetic field lines are pointing in opposite directions, giving the form of non-uniform field depicted.

The work will be to see if such confined states in this field are indeed theoretically feasible along with exploring the energy quantisation of such states and associated wavefunctions. Then work will be done to investigate any emergent physical effects due to these properties of the electrons, so that predictions may be made about experimental observables which may be used in later works to validate the existence of any confined states found.

4 Conclusion

To summarise the structure of graphene gives rise to regions of linear dispersion near the \vec{K} and \vec{K}' points called Dirac cones. In these low energy regions the electrons in graphene behave as light-like, relativistic particles, moving at the Fermi velocity called massless Dirac Fermions, with wavefunctions of the forms of spinors. These particles exhibit the Klein tunneling phenomenon where relativistic particles cannot be confined using the standard method of potential barriers, causing possible limitations to graphene-based nanoscience applications. Magnetic fields provide a method of confinement using so-called snake states. Exploration of the effect of a non-uniform magnetic field due to a uniform current loop on the dynamics of massless Dirac fermions will be conducted, and subsequent work will be performed to determine the Landau quantisation of particles in such a field to make predictions of any resultant measurable physical properties so that the validity of the results of this work may be determined.

References

- [1] Wallace, P. R., “The Band Theory of Graphite”, Physical Review, 71(9), 622–634, (1947)
- [2] Novoselov, K. S.; Geim, A. K.; Morozov, S. V.; Jiang, D.; Zhang, Y.; Dubonos, S. V.; Grigorieva, I. V.; Firsov, A. A., “Electric Field Effect in Atomically Thin Carbon Films”, Science 306 (5696): 666–669, (2004)
- [3] Katsnelson, M., Novoselov, K. & Geim, A., “Chiral tunnelling and the Klein paradox in graphene”, Nature Phys 2: 620–625, (2006).
- [4] Web Resource: Fuchs. J, Goerbig. M; “Introduction to the Physical Properties of Graphene”; http://web.physics.ucsb.edu/~phys123B/w2015/pdf_CoursGraphene2008.pdf
- [5] Grossso. G, Pastori Parravicini. G, ”Solid State Physics”, 2nd Edition, Academic Press, (2014), Pg55
- [6] Inagaki. M.; Kang. F.; Toyoda. M.; Konno. H., “Advanced Materials Science and Engineering of Carbon”, Butterworth-Heinemann: 41-42 (2014)
- [7] Grosso. G.; Pastori Parravicini. G., “Solid State Physics”, 2nd Edition, Academic Press: 182 (2014)
- [8] Katsnelson. M., “Graphene: Carbon in Two Dimensions”, Cambridge University Press: 9, (2012)
- [9] “Superconductors: Dirac cones come in pairs”, Tohoku University Advanced Institute for Materials Research - Research Highlights, (2011). https://www.wpi-aimr.tohoku.ac.jp/en/aimresearch/highlight/2011/20110829_000812.html (Accessed 06/03/2020)
- [10] Castro Neto A. H.; Guinea F.; Peres N. M. R.; Novoselov K. S.; Geim A. K., “The electronic properties of graphene” Rev. Mod. Phys. 81, 109, (2009)
- [11] Novoselov, K. S.; Geim, A. K.; Morozov, S. et al, “Two-dimensional gas of massless Dirac fermions in graphene”, Nature 438, 197–200, (2005)
- [12] Banks. T, “Modern Quantum Field Theory: A Concise Introduction”, Cambridge University Press: 45 (2012)
- [13] Dirac P. A. M.; Fowler R. H., “The quantum theory of the electron”, 117. Proc. R. Soc. Lond. A (1928)
- [14] Klein, O, “Die Reflexion von Elektronen an einem Potentialsprung nach der relativistischen Dynamik von Dirac”, Zeitschrift für Physik. 53 (3–4), (1929)
- [15] Stander N.; Huard B.; Goldhaber-Gordon D, “Evidence for Klein Tunnelling in Grahene p-n junctions”, Phys. Rev. Lett. 102 026807, (2009)
- [16] Katsnelson. M, “Graphene: Carbon in Two Dimensions”, Cambridge University Press: 24, (2012),
- [17] Landau. L; Lifshitz. E, “A course in theoretical physics: quantum mechanics” (Non-relativistic theory), Translated by Sykes J. B.; Bell J. S., 3rd Edition, Butterworth-Heinemann: 458, (1981)
- [18] Ferry. D. “Transport in Semiconductor Mesoscopic Devices”, IOP Publishsing Ltd: 6-4, (2015)
- [19] Williams, J. R.; Marcus C. M., “Snake States along Graphene p-n Junctions.”, Phys. Rev. Lett. 107.4: 046602, (2011)
- [20] Liu Y.; et al. “Snake states and their symmetries in graphene.”, Phys. Rev. B 92.23: 235438, (2015)
- [21] Ghosh T. K.; et al, “Conductance quantization and snake states in graphene magnetic waveguides.” Phys. Rev. B 77.8: 081404, (2008)
- [22] Oroszlány L.; et al, “Theory of snake states in graphene.” Phys. Rev. B 77.8: 081403, (2008)